Materials Science Forum *Online: 2013-01-25*
ISSN: 1662-9752, Vols. 738-739, pp 518-524
doi:10.4028/www.scientific.net/MSF.738-739.518

Structure and properties of TiNi alloy subjected to severe plastic deformation and subsequent annealing

Belyaev Sergey[1], Drozdova Maria[1], Frolova Natalia[2], Pilyugin Vitaly[2], Resnina Natalia[1], Slesarenko Viacheslav[1, a] and Zeldovich Vitali[2]

[1]Saint-Petesburg State University, Saint-Petersburg, Russia

[2]Institute of Metal Physic, the Ural branch of RAS, Yekaterinburg, Russia

[a]slslesarenko@gmail.com

Keywords: shape memory alloys, martensitic transformations, severe plastic deformation, TiNi, high pressure torsion, annealing, differential scanning calorimetry.

Abstract. Processes, occurring on annealing of TiNi alloy, processed by high pressure torsion (HPT), were the focus of this research. Some peaks of heat release were found on heating the deformed samples up to 550 °C. If the initial structure of the alloy was amorphous (after 3.5 turns of HPT), then structural relaxation, crystallization and grain growth occurred on heating. When alloys had a crystalline structure (after rotation by 15 and 90 degrees), recovery, recrystallization and further grain growth took place on heating. It was observed that the TiNi alloy, subjected to 3.5 turns of HPT and subsequent heating up to 550 °C, underwent unusual kinetics of martensitic transformations. Austenite B2 phase transformed to martensite B19' phase following two transformation sequences B2→R→B19' and B2→ B19'.

Introduction

High pressure torsion (HPT) is a severe plastic deformation technique that is usually used to decrease the average grain size of alloys [1]. Application of this method for shape memory alloys (SMA) seems to be promising due to the strong dependence of martensitic transformation kinetics and functional properties on the grain size. Moreover, in [2] it has been reported that HPT may be used for the amorphization of TiNi alloys. In [2] transmission electron microscopy (TEM) showed that the structure of a TiNi alloy became amorphous after deformation under a pressure of 5 GPa to a true logarithmic strain of 7. However, amorphization was not complete and nanocrystals (average size <20 nm) and some medium-range-ordered debris (1-3 nm) may be found in the amorphous matrix [3]. SMAs demonstrate their unique mechanical properties due to martensitic transformations which occur in the crystalline state. This is why TiNi alloys with amorphous structure are not able to demonstrate shape memory effects. To form a crystalline structure in the alloy, samples subjected to HPT are usually heated up to a particular temperature to initiate the crystallization process. It is well-known that the characteristics of the crystalline structure such as grain size, grain distribution and phase composition are determined by the parameters of crystallization and other accompanying processes that occur on heating the alloy, for instance, structural relaxation, grain growth, etc [2–7]. Thus, to control crystalline phase formation, it is necessary to clearly understand the sequence of the processes taking place on heating of an amorphous alloy and the influence of these processes on the structure of the alloys and their properties.

The peculiarities of these processes, occurring during the continuous annealing of a TiNi alloy processed by high pressure torsion (HPT), are still not entirely clear due to the complexity of the experimental data interpretations. Some additional information may be found from the comparison of the thermal behavior of TiNi alloys with different structures after HPT (amorphous or crystalline). Moreover, the dependence of the kinetics of these processes on the heating rate makes it possible to estimate some important parameters such as, for instance, the activation energy. The focus of this work aimed to investigate heat release on heating TiNi alloys with different initial structures at different heating rates.

Experimental procedure

In the present study, a binary TiNi alloy with the nominal composition of Ti-50.2 at. %Ni was used. Round samples with a diameter of 5 mm were punched out of a TiNi sheet with a thickness of 0.55 mm. The samples initially were in B19' martensite phase at room temperature. These samples were divided into three sets. The samples from the first set were processed by HPT up to an angle of 15 degrees. The rotation angles for the second and the third sets were 90 and 1260 degrees, respectively. HPT was carried out at room temperature under a pressure of 8 GPa. The true logarithmic strain was calculated by the formula $\varepsilon=ln(\varphi r/l)$, where φ is the rotation angle, and r and l are the radius and the thickness of the sample, respectively. Therefore, the true strain was 0.87, 2.65 and 5.3 for the samples from the three sets, respectively. To study the processes occurring on heating, the samples were heated up to 550 °C at different heating rates 10, 20 and 40 °C/min in the chamber of a Mettler Toledo 822e differential scanning calorimeter. The martensitic transformations in the samples were studied by differential scanning calorimetry (DSC) on cooling and heating in the temperature range of 120 ÷ -100 °C at a heating/cooling rate of 10 °C/min. The onset (T_s) and peak (T_p) temperatures were determined according to the ASTM standard test method F 2004-00. The crystal structure was revealed by X ray analysis with Cu K_α radiation at a temperature of 120 °C in which the crystalline structure of the alloy was in the austenite B2 phase. TEM was used to study the structure of deformed samples. The foil for TEM was cut off at a distance $r/2$ from the center of the sample. TEM was performed using a JEM 200CX electron microscope at a voltage of 160 kV.

Results and discussion

Structure of the TiNi alloy subjected to HPT

The TEM results showed that samples subjected to deformation up to 15 degrees kept their crystalline structure while the samples subjected to deformation up to 1260 degrees (3.5 turns) became amorphous. At the same time fine nanograins (average size 8-25 nm) remained in amorphous matrix after deformation up to 1260 degrees (Fig. 1a, b). These data are in a good agreement with [6]. The samples deformed up to 90 degrees were characterized by a crystalline structure with an average grain size of 10-30 nm (Fig. 1c, d). The greatest volume fraction of the crystalline phase was in B2 phase (right vertical arrow) while some volume of the crystalline phase was in the martensite B19' phase (left vertical and oblique arrows). Moreover, a small amount of the amorphous phase was observed (diffusion ring marked by horizontal arrows). Thus, the samples from the different sets had different structures.

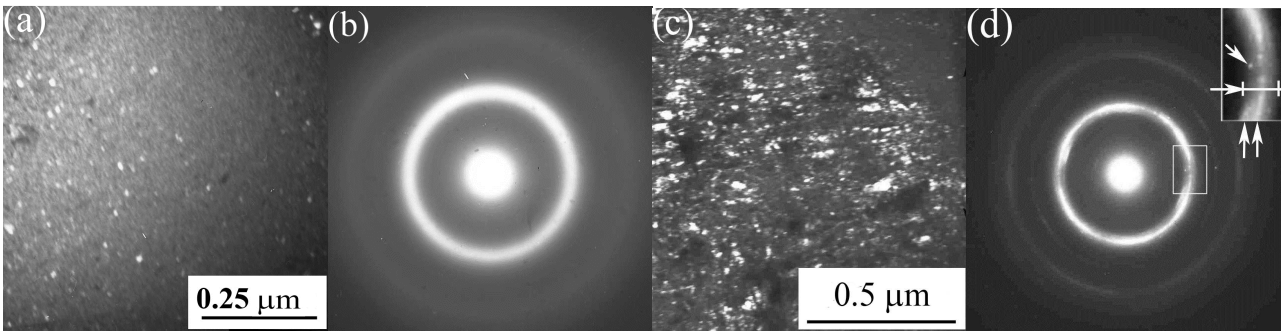

Figure 1. Dark-field TEM micrograph (a, c) and SAED patterns (b, d) for the sample, deformed up to 90 (c, d) and 1260 (a, b) degrees.

Heat release on heating the samples subjected to HPT

As was shown above, the samples deformed up to 1260 degrees were characterized by an amorphous structure. According to [8] several processes may occur in amorphous alloys on heating: structural relaxation, glass transition, crystallization and grain growth. Fig. 2 presents the DSC curves, obtained on heating the samples deformed up to 1260 degrees at the heating rates of 10, 20 and 40 °C/min. Three exothermal peaks were observed regardless of the heating rate. For all heating rates, the peak temperatures and enthalpies are shown in Tables 1 and 2. There was no evidence of glass transition observed on DSC curve. The low temperature peak (P_1) was characterized by relatively low enthalpy in comparison with the enthalpy of peak P_2 observed at higher temperatures. It is well-known that structural relaxation in amorphous alloys usually precedes the crystallization. Structural relaxation starts at room temperature and takes place at a wide temperature range till crystallization start. The analysis of the parameters of the DSC peaks showed that the first peak (P_1) corresponds to such conditions. This peak was characterized by small enthalpy and was observed at a wide temperature range. For instance, on heating at 10 °C/min, the enthalpy of P_1 was 2.8 J/g, and the temperature range was from 105 °C to 192 °C. This allows one to conclude that first peak (P_1) corresponds to structural relaxation.

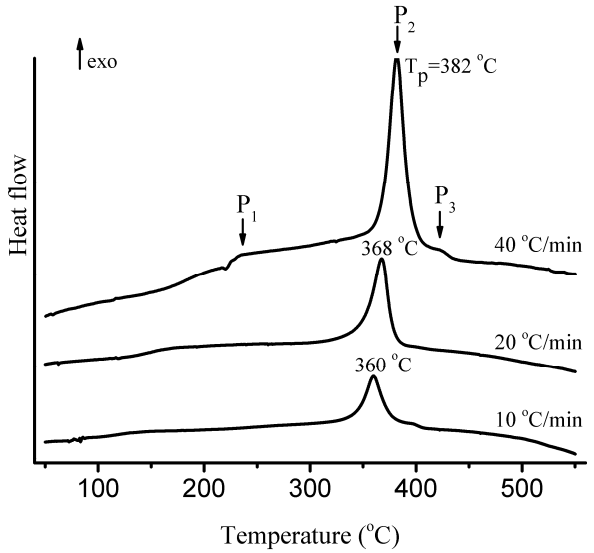

Figure 2. DSC curves, obtained on heating up to 550 °C at heating rates of 10, 20 and 40 °C/min of the sample deformed up to 1260 degrees.

Table 1. Parameters (start and peak temperatures T_s, T_p and enthalpy H) of the first calorimetric peak P_1 observed on heating up to 550 °C with several heating rates and the activation energy E_a estimated by the Kissinger method (on the basis of T_p).

Heating rate	10 [°C/min]		20 [°C/min]		40 [°C/min]		
Rotation angle	T_s (T_p) [°C]	H [J/g]	T_s (T_p) [°C]	H[J/g]	T_s (T_p) [°C]	H [J/g]	E_a [kJ/mol]
15	107 (139)	1.1	117 (159)	2.0	120 (176)	1.1	51
90	106 (140)	2.0	115 (151)	2.3	161 (203)	1.4	25
1260	105 (145)	2.8	132 (171)	3.1	153 (235)	4.8	5.5

The second DSC peak (P_2) was characterized by an enthalpy of 32.8 J/g and was observed in a relatively narrow temperature interval. An increase in the heating rate resulted in an increase in peak temperature. Comparison of the peak temperatures, found on the DSC curves obtained at different heating rates, made it possible to estimate the activation energy of this process by Kissinger's method on the basis of T_p measurements. This value was equal to 222 kJ/mol, which is in good agreement with the value of the activation energy, corresponded to the crystallization of an amorphous alloy [9]. Therefore, the second peak (P_2) was caused by crystallization. The crystallization temperature in this sample was 100 °C lower in comparison with temperature of $Ti_{50}Ni_{25}Cu_{25}$ melt-spun ribbons [3]. Such a significant difference between the crystallization temperatures is caused by the difference in the amorphous state of the HPT samples and the melt-spun ribbons. It is known that in an amorphous state obtained by severe plastic deformation, some nanocrystals and medium-range-ordered debris (1-3 nm) which survived the HPT deformation remain in the amorphous matrix. These inclusions may act as centres of crystallization and result in

a decrease in the crystallization temperature [6]. There was one more peak (P_3) observed on the DSC curve; it was accompanied by lower heat release in comparison with P_1 and P_2, and was obviously caused by some exothermal process, occurring just after the completion of crystallization, but its nature will be discussed later.

Table 2. Parameters (start and peak temperatures T_s, T_p and enthalpy H) of the second calorimetric peak P_2 observed on heating up to 550 °C with several heating rates and the activation energy E_a estimated by the Kissinger method (on the basis of T_p)

Heating rate	10 [°C/min]		20 [°C/min]		40 [°C/min]		
Rotation angle	T_s (T_p) [°C]	H [J/g]	T_s (T_p) [°C]	H[J/g]	T_s (T_p) [°C]	H [J/g]	E_a [kJ/mol]
15	236 (334)	7.0	270 (343)	5.8	277 (348)	4.7	283
90	270 (344)	10.0	277 (354)	9.7	298 (361)	9.2	251
1260	336 (360)	32.8	341 (368)	25.6	359 (382)	22.2	222

There were three exothermal peaks, observed on the DSC curves obtained on heating the samples deformed up to 15 and 90 degrees with a heating rate of 20 °C/min (Fig. 3). One may see that the number of peaks and the ratio of their intensities were similar in the amorphous and crystalline states (compare Fig. 2 and Fig. 3). At the same time, it is obvious that the nature of these processes, accompanied by heat release on heating, must be different in samples with amorphous (1260 degrees) and crystalline (15 and 90 degrees) structures.

Energy, expended in severe plastic deformation, is stored in the material as strain energy associated with various defects created by the deformation [10]. HPT not only leads to grain refinement, but is also able to increase the density of dislocations. This results in the accumulation of elastic energy in the alloy, which may be released during subsequent annealing [10]. In a polycrystalline alloy, phase solution, recovery, recrystallization and grain growth may occur during heating. As the chemical composition of the studied alloy was Ti-50.2 at. %Ni, no phase solution may take place on heating [11]. Thus, during heating of preliminarily deformed Ti-50.2 at. %Ni, only recovery processes, recrystallization and grain growth may occur. Among these three processes, the recovery process takes place at the lowest temperatures, followed by recrystallization and grain growth. This process starts at room temperature and takes place over a wide temperature range. The first peak on the DSC curves occurred at a very wide temperature range of 110-225 °C; hence, one may conclude that this heat release is due to the recovery process.

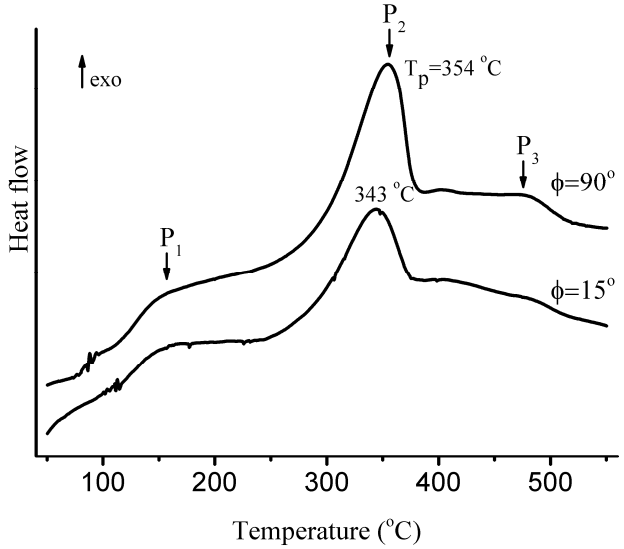

Figure 3. DSC curves, obtained on heating up to 550 °C of the sample deformed up to 15 and 90 degrees at heating rate 20 °C/min

Usually the recovery process, including relaxation and polygonization, is a precursor of the recrystallization of a deformed alloy. Recrystallization leads to the formation of new defect-free grains instead of the deformed ones by a nucleation and growth process. This process is accompanied by considerable energy release. Thus, one may conclude that the second peak (P_2) was caused by this process. Moreover, with greater preliminary deformation of the alloy, a more intensive process of recrystallization occurs. A comparison of the data presented in Table 2 shows

that the enthalpy of the second peak (P_2), measured in the sample subjected to deformation up to 15 degrees, was approximately two-fold lower than the same value measured in the sample subjected to deformation up to 90 degrees.

A third peak (P_3) was found on the DSC curves, obtained on heating the samples subjected to deformation up to 15 and 90 degrees. As mentioned above, the same peak was also observed in the sample deformed up to 1260 degrees. The process that corresponds to this peak takes place when crystallization or recrystallization is complete, so this peak may be caused by grain growth. However, this should be clarified by other structural experiments, which will be carried out later.

Therefore, according to the data obtained in this study, the sequence of the processes that occur on heating depends on the initial structure of the alloy. If the alloy's structure is amorphous after HPT, structural relaxation, crystallization and the further grain growth take place sequentially. In the case where the structure of the alloy is crystalline, recovery, recrystallization and grain growth occur on heating. These assumptions were verified by the data from special experiments where the preliminarily deformed samples were heated up to 550°C with intermediate interruptions at different temperatures. TEM and electroresistivity measurements were carried out after each interruption. These results will be published elsewhere.

Martensitic transformations in the samples subjected to HPT and heating up to 550 °C

Heating and cooling of the all HPT-processed samples in the temperature range of 120 ÷ -100 °C revealed that martensitic transformations were suppressed after deformation. As expected, heating of the preliminarily deformed samples up to 550 °C restored the ability of the alloy to undergo martensitic transformation. Fig. 4 presents the DSC curves obtained on cooling (a) and heating (b) of the samples, deformed up to 15, 90 and 1260 degrees and subjected to subsequent heating up to 550 °C. In the samples deformed up to 15 and 90 degrees, two exothermal peaks were observed on cooling and one peak on heating. Special experiments, where thermal cycling of the alloy has been carried out in the temperature range of the incomplete forward martensite transformation, showed that the two calorimetric peaks observed on cooling were due to B2→R→B19' transformations and the single calorimetric peak observed on heating was caused by B19'→ B2 transformation.

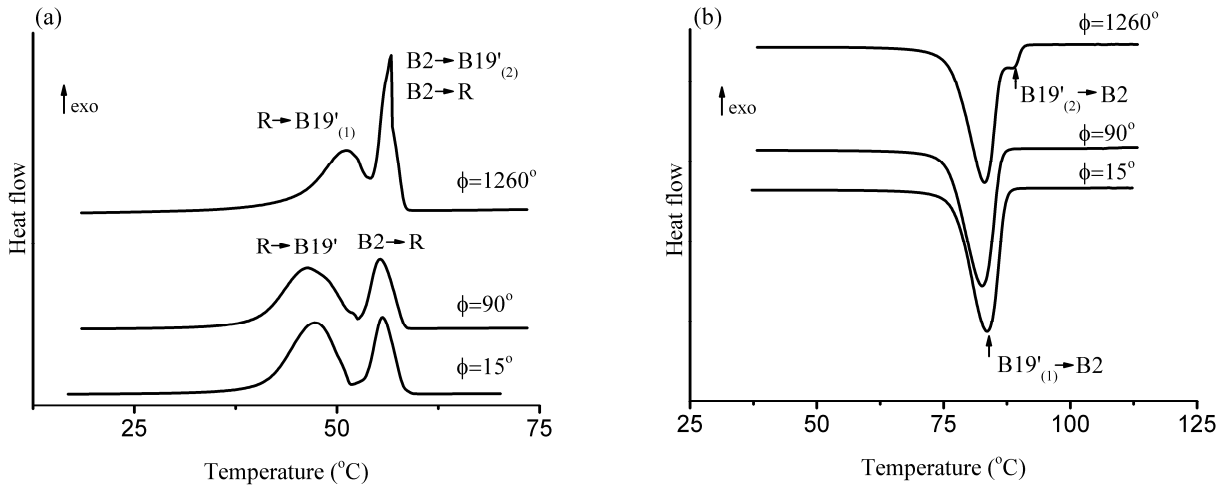

Figure 4. DSC curves, obtained on cooling (a) and heating (b) of the samples, deformed up to 15, 90 and 1260, in the temperature range of 120 ÷ -100 °C with heating rate of 10 °C/min

In the sample deformed up to 1260 degrees and heated up to 550 °C, two peaks were observed on cooling. Thermal cycling in the temperature range of the incomplete forward martensite transformation allowed one to determine that the first calorimetric peak consisted of two overlapping peaks and that these peaks were due to B2→R and B2→B19' transitions; the second calorimetric peak was due to the R→B19' transformation. Thus, in the TiNi alloy subjected to deformation up to 1260 degrees and subsequent heating up to 550 °C, the austenite phase B2

transformed into the martensite phase B19' by two pathways simultaneously. The first way was B2→R→B19' transition and the second was a direct B2→B19' transition without the formation of the intermediate R phase. As it was found in [12], B19' phase, obtained in different ways, transformed to B2 phase on heating at different temperature ranges. This resulted in the observation of two calorimetric peaks on heating (Fig. 4b). Thus, the TiNi alloy after HPT up to 1260 degrees and subsequent heating up to 550 °C contained various volumes capable of undergoing different sequences of direct martensitic transformation on cooling. This was probably due to differences in the grain parameters and/or a heterogeneous distribution of internal stresses. This will be precisely clarified in further studies.

Conclusion

1. Heating a TiNi alloy with amorphous structure, induced by HPT, results in the observation of three exothermal processes which occur due to structural relaxation of the amorphous phase, crystallization and grain growth.
2. Heating a TiNi alloy in which the crystalline structure has not been destroyed by HPT leads to the observation of three calorimetric peaks, which are caused by the recovery processes, recrystallization and grain growth.
3. B2→R→B19' direct martensitic transformations and the reverse B19'→B2 transformation are found on cooling and heating the TiNi alloy, subjected to HPT up to 15 and 90 degrees and subsequent heating.
4. Heating a TiNi alloy with amorphous structure, induced by HPT, results in the formation of various volumes of the crystalline phase. These volumes undergo different types of martensitic transformations, B2→R→B19' or B2→B19'. It is likely that such kinetics is caused by differences in grain parameters and/or a heterogeneous distribution of internal stresses.

References

[1] A. Zhilyaev and T. Langdon, Using high-pressure torsion for metal processing: Fundamentals and applications, Progress in Materials Science, vol. 53 (2008), no. 6, pp. 893–979.

[2] A. Sergueeva, C. Song, R. Valiev, and A. Mukherjee, Structure and properties of amorphous and nanocrystalline NiTi prepared by severe plastic deformation and annealing, Materials Science and Engineering: A, vol. 339 (2003), no. 1–2, pp. 159–165.

[3] M. Peterlechner, T. Waitz, and H. P. Karnthaler, Nanocrystallization of NiTi shape memory alloys made amorphous by high-pressure torsion, Scripta Materialia, vol. 59 (2008), no. 5, pp. 566–569.

[4] M. Peterlechner, J. Bokeloh, G. Wilde, and T. Waitz, Study of relaxation and crystallization kinetics of NiTi made amorphous by repeated cold rolling, Acta Materialia, vol. 58 (2010), no. 20, pp. 6637–6648.

[5] R. Singh, H. Rösner, E. A. Prokofyev, R. Z. Valiev, S. V. Divinski, and G. Wilde, Annealing behaviour of nanocrystalline NiTi (50 at% Ni) alloy produced by high-pressure torsion, Philosophical Magazine, vol. 91 (2011), no. 22, pp. 3079–3092.

[6] T. Waitz, V. Kazykhanov, and H. P. Karnthaler, Martensitic phase transformations in nanocrystalline NiTi studied by TEM, Acta Materialia, vol. 52 (2004), no. 1, pp. 137–147.

[7] V. G. Pushin, V. V. Stolyarov, R. Z. Valiev, T. C. Lowe, and Y. T. Zhu, Nanostructured TiNi-based shape memory alloys processed by severe plastic deformation, Materials Science and Engineering: A, vol. 410–411 (2005), pp. 386–389.

[8] C. Syryanarayana and A. Inoue, Bulk Metallic Glasses. CRC Press, 2011, pp. 188–264.

[9] K. Inaekyan, V. Brailovski, S. Prokoshkin, A. Korotitskiy, and A. Glezer, Characterization of amorphous and nanocrystalline Ti–Ni-based shape memory alloys, Journal of Alloys and Compounds, vol. 473 (2009), no. 1–2, pp. 71–78.

[10] R. Abbaschian, L. Abbaschian, and R. Reed-Hill, Physical Metallurgy Principles. fourth edition, Cengage Learning, 2008, pp. 216–250.

[11] K. Otsuka and X. Ren, Physical metallurgy of Ti–Ni-based shape memory alloys, Progress in Materials Science, vol. 50 (2005), no. 5, pp. 511–678.

[12] N. Resnina and S. Belyaev, Multi-stage martensitic transformations induced by repeated thermal cycling of equiatomic TiNi alloy, Journal of Alloys and Compounds, vol. 486 (2009), pp. 304–308.